RESULTS OF THE IAASS RE-ENTRY ANALYSIS TEST CAMPAIGN 2012

T. Lips[1], I. Huertas[2], S. Ventura[3], and P. Omaly[4]

[1]*HTG GmbH, Max-Planck-Str. 19, 37191 Katlenburg-Lindau, Germany, Email: t.lips@htg-hst.de*
[2]*ESA/ESTEC, Keplerlaan 1, 2200 AG Noordwijk, Netherlands, Email: irene.huertas@esa.int*
[3]*ESA/ESTEC, Keplerlaan 1, 2200 AG Noordwijk, Netherlands, Email: sergio.ventura@esa.int*
[4]*CNES, 18 Avenue Édouard Belin, 31400 Toulouse, France, Email: pierre.omaly@cnes.fr*

ABSTRACT

The Fourth IAASS Launch and Re-entry Safety Workshop was held at the NASA Wallops Flight Facility in September 2012. This was a joint workshop of the two IAASS Technical Committees for Space Hazards and Launch Range Safety. Since the second workshop in 2010, re-entry analysis test campaigns became a regular activity of these workshops. The purpose of these test campaigns is to promote cooperation, collaboration, and data exchange between the operators and developers of re-entry analysis tools all around the world in order to achieve a common baseline for reliable on-ground risk prediction due to surviving fragments from re-entering spacecraft. Two test cases were selected for the IAASS Re-entry Analysis Test Campaign 2012: an artificial, simplified satellite (about 400 kg) and a Delta-II Second Stage (about 925 kg). The Delta-II case was a simulation of a historical re-entry event which occurred on January 22, 1997. Several fragments resulting from this re-entry event were recovered on US territory. This paper will summarize and discuss the re-entry analysis results of the Delta-II test case provided by the following tools: SCARAB, DEBRISK, SESAM, and ASTOS/DARS.

NOMENCLATURE

AOP	Argument of Perigee
AZM	Flight Azimuth (rel. to East direction, North positive)
DoF	Degrees of Freedom
FPA	Flight Path Angle (rel. to local horizon)
RAAN	Right Ascension of Ascending Node
TAN	True Anomaly
TLE	Two-Line Elements

1. INTRODUCTION

This paper is the first step of an ongoing mutual activity of the participants of the Fourth IAASS Launch and Re-entry Safety Workshop that took place in 2012. During this workshop, the Delta-II Second Stage re-entry, which occurred on January 22, 1997 (international designator 1996-024B, catalog no. 23852), was used as a reference case to compare re-entry predictions. Several fragments resulting from this re-entry event were recovered on US territory (see Fig. 1). Several tools were used to simulate this re-entry event: SCARAB, DEBRISK, SESAM, and ASTOS/DARS. More results are expected from other tools, and further sensitivity analysis will also be performed in the coming workshops.

The goal of this comparison was two-fold. Firstly, the comparison of the results permits a comparison of the methodology of the tools. Secondly, it was interesting to compare the assumptions each tool and tool user took when performing a re-entry analysis. A comparison of both points may provide areas of improvement of the re-entry risk analysis methodology. This paper will summarize and discuss the re-entry analysis results of the Delta-II test case provided by the mentioned tools.

Figure 1. Delta-II Second Stage - Recovered Fragments (Credit: NASA, Tulsa World, Aerojet)

2. ANALYSIS TOOLS

2.1. SCARAB

SCARAB (Spacecraft Atmospheric Re-Entry and Aerothermal Break-Up) is a spacecraft-oriented software tool allowing the analysis of mechanical and thermal destruction of spacecraft and other objects during re-entry (controlled or uncontrolled). It is an integrated software package (six degrees-of-freedom flight dynamics, aerodynamics, aerothermodynamics, thermal- and structural analysis) used to perform re-entry risk assessments (quantification, characterization and monitoring of surviving fragments during re-entry). The software application has been validated with in-flight measurements, re-entry observations and wind tunnel experiments, and it has been compared to other re-entry prediction tools of the international community.

SCARAB has been developed under ESA/ESOC contracts since 1995 under the lead of HTG (Hypersonic Technology Göttingen) and with support from other European and international partners. It is considered as operational software. The software development has evolved over time, based on lessons learned from preceding software versions, upgrades and specific re-entry analyses performed for various satellites (e.g. ROSAT, BeppoSAX, TerraSAR-X, GOCE, Sentinel-2/3, SWARM), and for the ATV and the ESA launcher programs. Typical launch vehicle (or similar) re-entry applications have been: Ariane-5 stages (EPC, EPS/VEB, ESC-A), Vega stages (Zefiro-9, AVUM), and ATV.

SCARAB version 3.1L [1] has been used for this paper.

2.2. SESAM

HTG has also developed SESAM (Spacecraft Entry Survival Analysis Module), a module of the ESA DRAMA (Debris Risk Assessment and Mitigation Analysis) software [2]. SESAM is an object-oriented re-entry analysis code based on a user-defined fragment list of simple shaped objects (sphere, box, cylinder, flat plate) which are released at an also user-defined breakup altitude. SESAM is able to perform re-entry analysis with the following features: random tumbling attitude of the spacecraft; break-up at fixed altitude (78 km as default); material properties not depending on temperature; aerodynamic drag and aerothermodynamic heating coefficients as in NASA's ORSAT 5.0 (Object Reentry Survival Analysis Tool, [3]).

SESAM version 1.1a has been used for this paper.

2.3. ASTOS/DARS

ASTOS (AeroSpace Trajectory Optimization Software) is a tool developed by ASTOS Solutions GmbH and ESA/ESTEC for simulation and optimization of spacecraft trajectories. In particular, ASTOS has the module DARS (Debris Analysis for Re-entry Spacecraft) for casualty re-entry analysis. The tool has been developed at ESA-ESTEC and analyzes the atmospheric re-entry of spacecraft or the different stages of launcher vehicles [4]. DARS is an object-oriented code based on a user defined fragment list of primitive-shaped objects (sphere, box, cylinder, flat plate), which can be released at user-defined breakup altitudes. Through a trajectory propagator and an aerothermal module, DARS supplies the trajectory and the thermal state of each fragment. It is able to determine if the object will reach the surface of the planet or if it will demise on its path through the atmosphere. If the object reaches the surface of the planet, DARS computes the energy at the impact point and provides the necessary data to calculate the probability of casualty and fatality to perform a risk analysis for the re-entry. Additional outputs such as shape, position and dimensions of the footprint are computed by ASTOS [5].

For this paper, ASTOS version 7.0.3 was used with the following features: random tumbling attitude of the spacecraft; break-up at fixed altitude (78 km); material properties independent of temperature; aerodynamic drag and aerothermodynamic heating coefficients defined as in NASA's ORSAT 5.0 [3].

2.4. DEBRISK

CNES has developed the engineering tool DEBRISK [6] which allows the operator to simulate space object re-entry phase. DEBRISK gives the 3D trajectory of re-entering satellite components as well as the surface heat load , debris demise altitude, or impact energy of the individual survival fragments. It is based on a direct approach object in which the space vehicle is represented by a set of interconnected basic geometries (spheres, boxes, flat plates, and cylinders). A structure of type parent-child allows to define the relations between these various objects. Every object is defined by its shape, its sizes, its mass and its material (most common satellite materials are available in the database). During the descent, the wall heat loads are integrated to obtain the surface temperature. In case of surface melting, layers of material are peeled-off and the shape and trajectory are updated until demises occur. The software supplies a list of the surviving objects and their characteristics upon arrival ground.

DEBRISK version 2.04.10 has been used for this paper.

3. TEST CASE

The Delta-II Second Stage re-entry which occurred on January 22, 1997, has been used as test case for the IAASS Re-entry Analysis Test Campaign 2012. Several fragments resulting from this re-entry event were recovered on US territory. Design information available from [3, 7], other public web sources (e.g. images), and some engineering assumptions have been used to define this test case.

Tab. 1 shows the overall mass budget of the Delta-II Second Stage. Figs. 2 and 3 show a photograph of the stage and a derived sketch with dimensions. Fig. 4 shows the SCARAB model which has been created based on these data, and Tab. 2 includes the fragment list which has been used by SESAM, ASTOS/DARS, and DEBRISK. The corresponding material properties are listed in Tab. 3.

Table 1. Delta-II Mass Budget

Subsystem	Mass [kg]
Engine	198
Gas Tanks	81
Guidance Section	165
Payload Adapter	20
Propellant Tank	267
Structure	193
Total	**924**

The initial conditions for this test case have been derived from the actual last TLE data set (Tab. 4, www.space-track.org). The TLE have been transformed into osculating Kepler elements by using the SGP4 method [8]. Osculating Kepler elements and corresponding geodetic parameters are shown in Tab. 5.

Table 5. Initial Conditions for Delta-II Second Stage 1996-024B

Kepler Elements*	
Date [dd.mm.yyyy]	22.01.1997
Time, GMT [hh:mm:ss]	09:02:32.420
Semi Major Axis [km]	6495.30524
Eccentricity	0.002241
Inclination [deg]	96.57158
RAAN [deg]	344.69854
AOP [deg]	98.30452
TAN [deg]	262.00864
Geodetic Parameters†	
Altitude [km]	119.16050
Latitude [deg]	0.31315
Longitude [deg]	87.27374
Velocity [km/s]	7.89959
FPA [deg]	-0.12407
AZM [deg]	99.98748

*used by SCARAB, DEBRISK
†used by SESAM, ASTOS/DARS

4. RESULT COMPARISON

All tools have provided a wide set of output data, in the native formats of the tools. A common template was also used to facilitate the comparison of results. The test case was analyzed for all the fragments generated during re-entry, including ablation phenomena and demise, ground impacts and footprint prediction. This paper concentrates on the main propellant tank results, focusing on the trajectory and temperature evolution.

4.1. Trajectories

The initial conditions in Tab. 5 were inserted in the four tools for propagation of the trajectory, as can be seen from Fig. 5. The entry interface is located just North of the ascending node of the orbit, and South to the Bay of Bengal. The atmospheric trajectory propagates in all tools until the stage reaches the North-American continent.

The ground distance covered by the fragments differs in the different tools. The shortest downrange is computed by SESAM and DEBRISK, with a covered distance between 12,000 km and 13,000 km. ASTOS follows next with a re-entry at about 17,000 km downrange and SCARAB has the longest computed re-entry with a ground track somewhat longer than 18,000 km.[1]
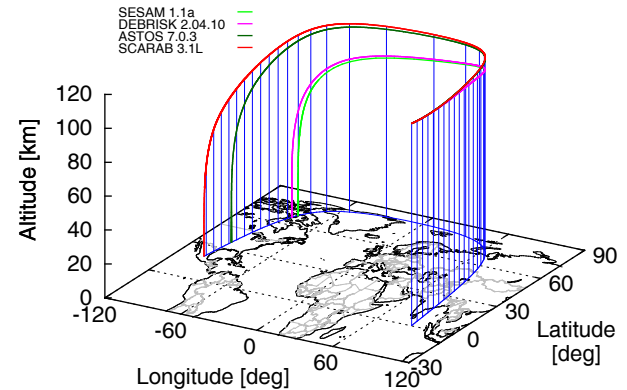
Figure 5. Re-entry Trajectory Parent/Main Object (Propellant Tank)

Similarities can be seen between SESAM and DEBRISK, and between SCARAB and ASTOS, respectively. The trajectory differences between both groups are caused already at high altitudes above 110 km. One reason for this effect can be that different atmosphere models are used by the tools. A second reason can be related to different aerodynamic implementations. Fig. 6 shows a very good agreement between the used atmosphere models using a logarithmic scale for the atmospheric density. Fig. 7 applies a linear scale for the atmospheric density relative to the US-Standard 1976. This comparison shows that

---

[1]Fig.5 shows blue vertical tics every 500 km of covered downrange.
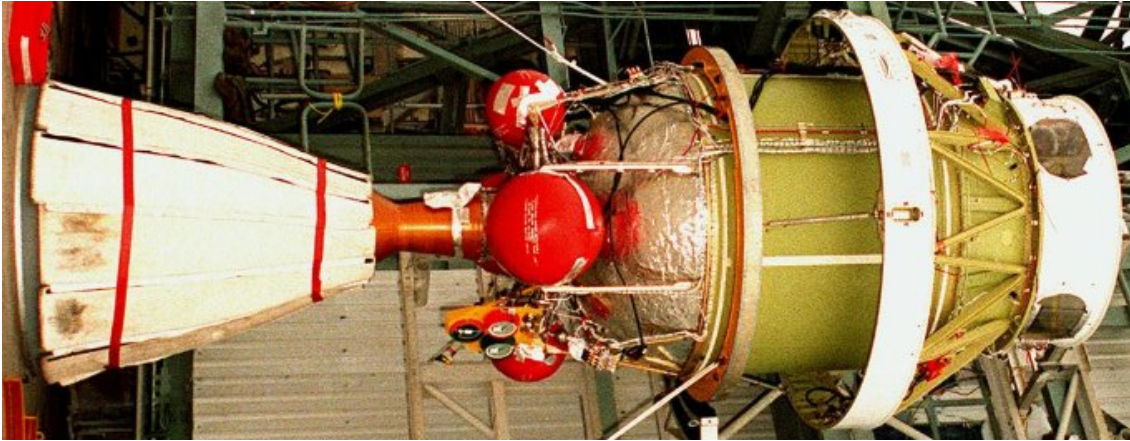
Figure 2. Delta-II Second Stage (Credit: NASA)
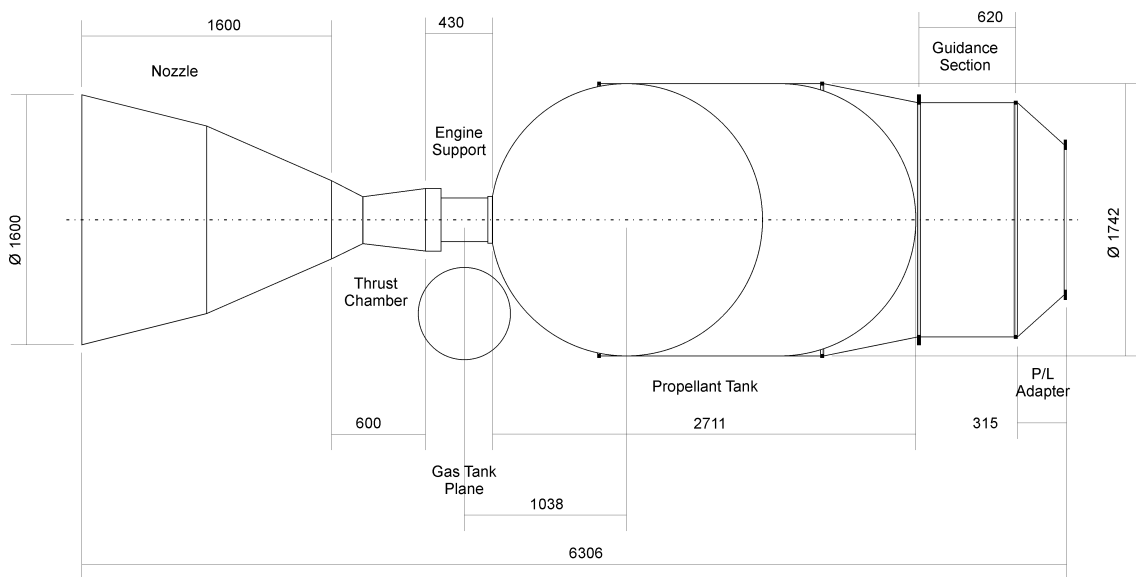
Figure 3. Delta-II Second Stage (derived sketch, dimensions in mm)
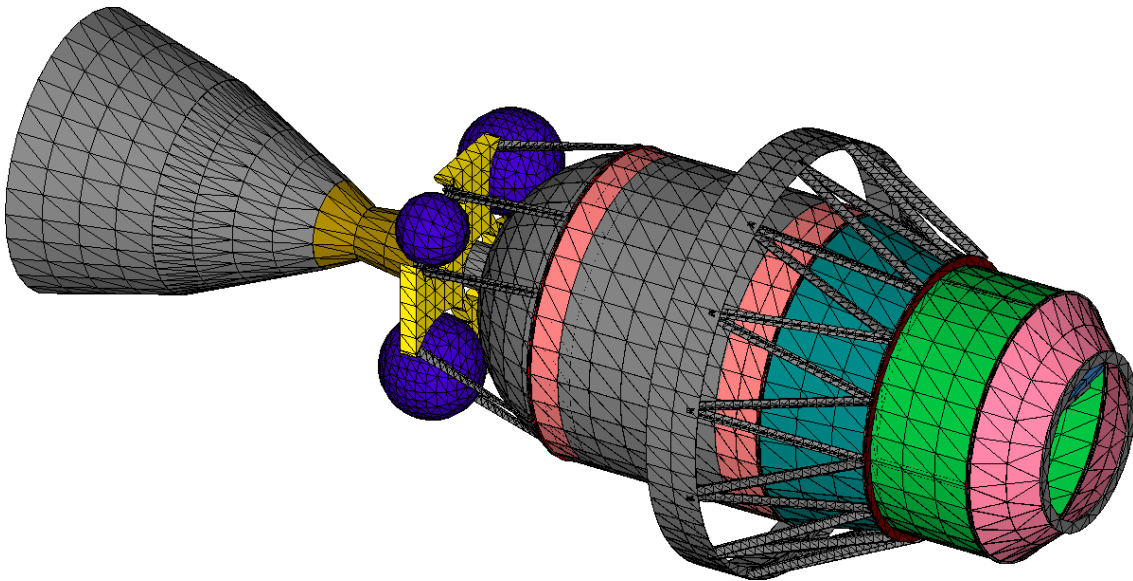
Figure 4. Delta-II Second Stage - SCARAB Model

Table 2. Fragment List for Delta-II Second Stage

Name	Shape	No. of fragments	Width/Diam. [m]	Length [m]	Height [m]	Mass [kg]	Material
Parent	Cylinder	1	1.8	6.3	0.0	924.343	-
PropTan	Cylinder	1	1.7	2.7	0.0	267.675	A316
ThrustC	Cylinder	1	0.44	0.6	0.0	45.8	Inconel
GasTan1	Sphere	2	0.41	0.0	0.0	10.056	TiAl6V4
GasTan2	Sphere	2	0.59	0.0	0.0	30.548	TiAl6V4
Nozzle	Cylinder	1	1.0	1.6	0.0	99.594	CFRP
EngSup	Cylinder	1	0.3	0.43	0.0	52.175	AA7075
GuideEl	Box	8	0.5	0.45	0.1	10.337	AA7075

Table 3. Material Properties

	SCARAB*	SESAM	ASTOS/DARS	DEBRISK
A316				
Melting Temperature [K]	1650	1650	1650	1644
Spec. Heat Capacity [J/kg/K]	460-715	611.5	611.5	460.6
Spec. Heat of Melting [kJ/kg]	274	274	274	286.098
Emissivity [-]	0.08-0.62	0.591	0.591	0.35
Inconel				
Melting Temperature [K]	1630	1570	1570	1571
Spec. Heat Capacity [J/kg/K]	420-830	673	673	435
Spec. Heat of Melting [kJ/kg]	309	309	309	311.664
Emissivity [-]	0.05-0.195	0.171	0.171	0.122
TiAl6V4				
Melting Temperature [K]	1873	1900	1900	1943
Spec. Heat Capacity [J/kg/K]	560-1100	746.4	746.4	807.5
Spec. Heat of Melting [kJ/kg]	400	400	400	393.559
Emissivity [-]	0.18-0.31	0.392	0.392	0.302
CFRP				
Melting Temperature [K]	700	700	700	2144
Spec. Heat Capacity [J/kg/K]	1100	1100	879	1257.55
Spec. Heat of Melting [kJ/kg]	16131.323	16131.323	0.2326	37.65
Emissivity [-]	0.78-0.8	0.86	1	1
AA7075				
Melting Temperature [K]	870	870	870	830
Spec. Heat Capacity [J/kg/K]	820-732	746.4	746.4	1012.35
Spec. Heat of Melting [kJ/kg]	385	385	385	376.788
Emissivity [-]	0.105-0.16	0.154	0.154	0.141

*Specific heat capacity and emissivity are temperature dependent parameters in SCARAB.

Table 4. Last Set of TLE for Delta-II Second Stage 1996-024B

```
1 23852U 96024B   97022.37676412  .99999999  24109-5  41939-3 0  4309
2 23852  96.5767 344.6986 0013684 128.9053 231.6615 16.61056074 42086
```

the relative differences between atmosphere models below 120 km altitude can be in the order of ±30%, depending on which atmosphere model is used as reference.

SCARAB[2] and ASTOS have used the MSISE-90 and the NRL-MSISE00 atmosphere models, respectively, with similar density profiles above 110 km altitude. Therefore, the trajectories provided by these two tools show a similar rate of descent, especially in the higher altitude regime. At lower altitudes, the different aerodynamic approach used by SCARAB, taking into account also aerodynamic stabilization of the tumbling motion, becomes a dominating source for the differences between SCARAB and ASTOS (i.e. 6-DoF versus 3-DoF propagation).

There is a very close agreement between the trajectories provided by SESAM and DEBRISK. However, a comparison between the US-Standard 1976 atmosphere model used by SESAM and the CIRA88-MSIS86 model used by DEBRISK shows the largest difference between all atmosphere models. Additional, currently unavailable output of SESAM's aerodynamic variables would be needed to further investigate this.
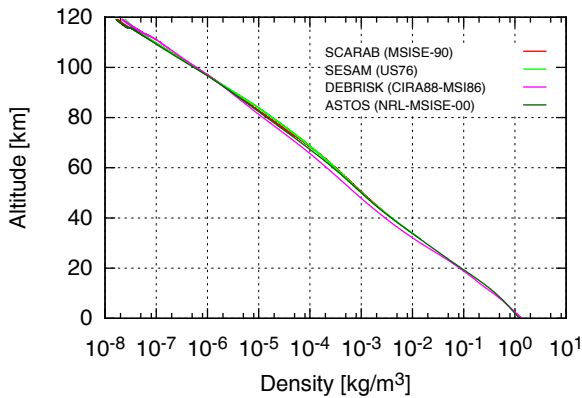
Figure 6. Atmospheric Density

Figs. 8 and 9 show a comparison of the velocity evolution along the trajectory. The first diagram somewhat disguises the relative differences (with respect to the SCARAB results) that are revealed in the second figure. The differences become significant after breakup at 78 km altitude, although SESAM, DEBRISK and ASTOS show the same quantitative development of values. Unexpected is the result of SESAM, especially the kink in velocity evolution at 78 km altitude which should not occur if the aerodynamic implementations inside SESAM, DEBRISK and ASTOS tools are identical.

At around 80 km altitude, SCARAB shows a sudden change is the velocity behavior. This change is caused by the loss of aerodynamic stability. Additionally, a sudden change in velocity profile can be observed in the transonic region of the other tools. This change can be explained

---

[2]SCARAB density output stops at Mach number 6, i.e. around 40 km altitude.
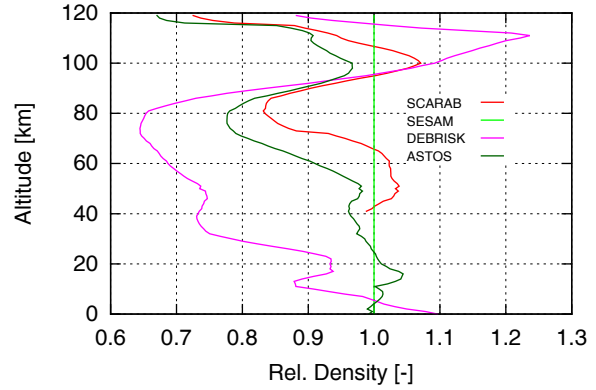
Figure 7. Relative Atmospheric Density (wrt. US Standard 76)
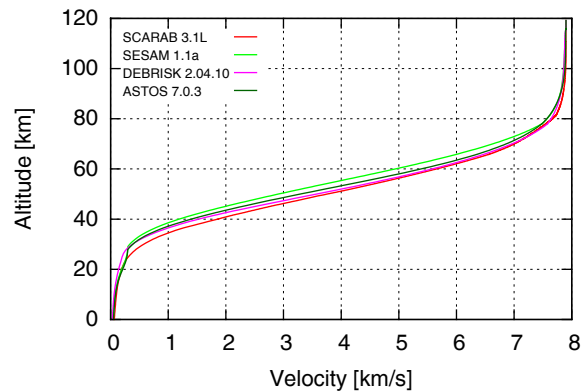
Figure 8. Velocity Parent/Main Object (Propellant Tank)

by a change of aerodynamic drag coefficients when decelerating to subsonic speeds.

There are several other factors that may affect the trajectory. The altitude of fragmentation in SESAM, DEBRISK and ASTOS is user-defined, whereas fragmentation in SCARAB is depending on thermal and structural conditions. The fragmentation of the objects being gradual, SCARAB is likely to use higher ballistic coefficients than other tools as a function of time for the main fragment. Also, primitive shapes' aerodynamic drag coefficients are defined with different values and flow conditions in each tool, causing a dissimilar deceleration drag. Furthermore, the material properties may be different, leading to different ablation rates, and thus to diverging ballistic coefficients.

4.2. Temperatures

A comparison of temperatures first requires some explanation on the SCARAB results. SCARAB does not provide one unique temperature for the modeled components of the re-entry object, but surface temperature distribu-
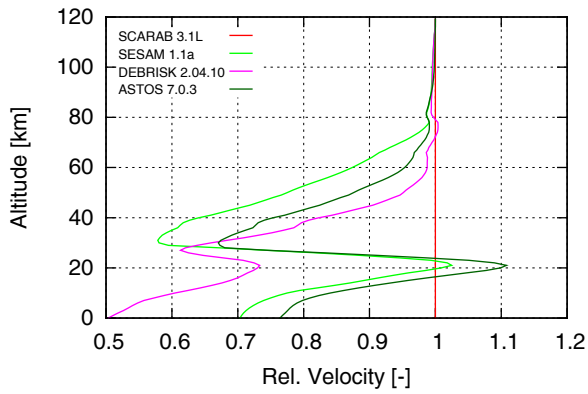
Figure 9. Relative Velocity Parent/Main Object (Propellant Tank; wrt. SCARAB)

tions at each time step of the simulation. Fig. 10 shows the temperature distribution of the main object at 65.5 km altitude. For comparison with the results of the other tools, mean and maximum temperatures have been extracted for the propellant tank at three positions: cylindrical section, and spherical tail (engine) and bow section. These results are shown in Figs. 11 and 12. Fig. 13 compares the temperature results from all tools for the propellant tank.
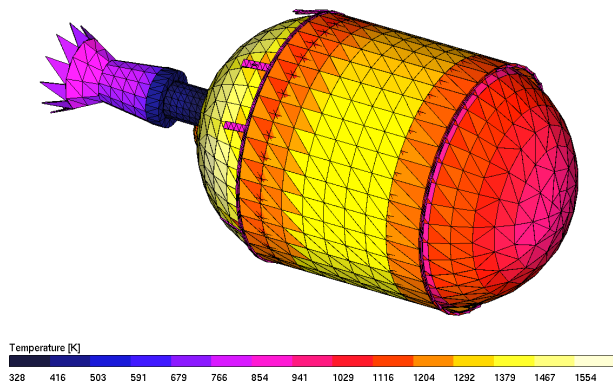
Figure 10. SCARAB Temperature Distribution (at 65.5 km altitude)

ASTOS, DEBRISK and SESAM make the assumption that a fragment is rotating such that a uniform, isotropic heat flux can be used, applying a lumped thermal mass model for the heating and melting process. The wall temperature of each fragment at the beginning of its propagation is user-defined input (300 K for this test case).

DEBRISK and ASTOS results show a good agreement, although the used material properties are different, especially for specific heat capacity and emissivity. It appears that the differences in material properties are compensated by the higher flight velocities and lower atmospheric densities calculated by DEBRISK. Differences in the implementation of the aerothermodynamic models are also possible, but have not yet been further analyzed.
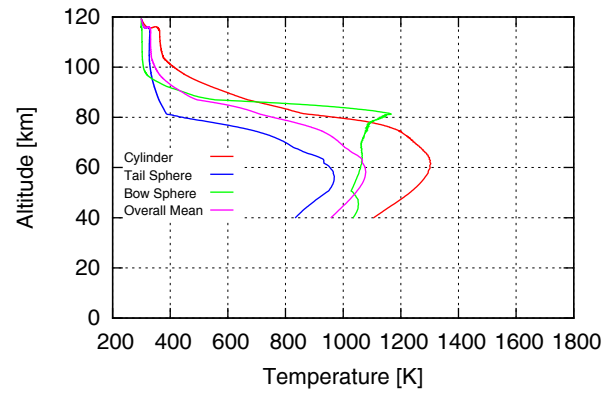
Figure 11. Mean Temperature Propellant Tank (SCARAB)
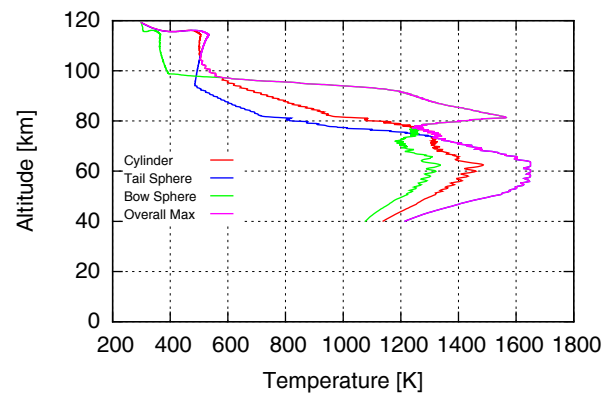
Figure 12. Max. Temperature Propellant Tank (SCARAB)

SESAM provides lower temperatures than DEBRISK and ASTOS. The material properties used by SESAM and ASTOS were identical. SESAM predicts lower velocities and higher atmospheric densities than DEBRISK and ASTOS at the altitude of peak heating around 60 km altitude. Especially the lower velocities appear to account for the lower temperatures predicted by SESAM. Again, differences in the applied aerothermodynamic models cannot be excluded.

The SCARAB results show first several effects that are not analyzed by the other tools. The heating begins already at higher altitudes before the breakup altitude of the other tools. The influence of solar radiation heating and cooling after entrance into the Earth's shadow can be seen at altitudes above 100 km. The temperature of the bow section of the tank becomes hotter than the other parts because of its dominant exposure to the flow until the aerodynamic stabilization is lost at around 80 km altitude. At lower altitudes, the propellant tank starts to tumble randomly.

In comparison to the results from the other tools, SCARAB predicts higher maximum temperatures, even reaching melting temperature at some locations of the
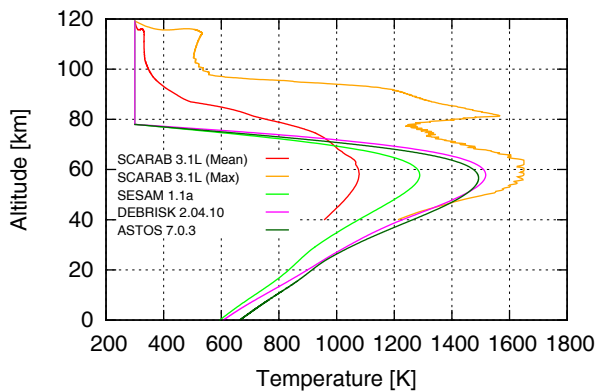
Figure 13. Temperature Parent/Main Object (Propellant Tank)

spherical tail section. The overall mean temperature of the complete propellant tank is lower than predicted by the other tools. Additionally, SCARAB underlines temperature fluctuations due to attitude motion, which influences the exposure of parts of the structure to the flow.

5.   SUMMARY, CONCLUSIONS, OUTLOOK

The benchmark test case based on the re-entry of the Delta-II Second Stage has permitted to make a first step in comparing technical details between re-entry analysis tools. The tools used in this comparison were SCARAB, SESAM, ASTOS, and DEBRISK. Differences in re-entry trajectory and temperature evolution results for the propellant tank have been identified. Differences in user inputs and tool settings have also been identified.

The identification of the reason for the differences in the results was difficult. It was observed that the tool users make different assumptions in certain inputs (e.g. atmosphere models, materials properties). It was also observed that some differences may arise from different implementations of aerothermodynamic and aerodynamic models inside the software. Because of this, it is very difficult to determine proper causal correlation between inputs, methods and the result variations. It is also possible that some factors have contradicting effects, and are ultimately not noticeable because they compensate each other.

For future comparisons, the number of parameters influencing the results should be limited. As much as possible, there should be a decoupling between the differences caused by inputs, and differences caused by the tools themselves. As a first step, it would be recommendable to harmonize the inputs (e.g. use the same atmospheric conditions and material database).

More results are expected from other tools during the Fifth IAASS Launch and Re-entry Safety Workshop in Montréal 2013. With the resulting discussion, it is foreseen that a revised benchmarking case will be proposed, together with a clear definition of the output content of the tools. Concentrating on simple geometric shapes (instead of a full spacecraft) could be beneficial to compare the tools' internal methods.

REFERENCES

1. Lips T., Fritsche B., Homeister M., et al., (2007). Re-entry Risk Assessment for Launchers - Development of the New SCARAB 3.1L, *Proceedings of the Second IAASS Conference*, ESA SP-645, ESA Communication Production Office, Noordwijk, The Netherlands

2. Martin C., et al., (2005). *Debris Risk Assessment and Mitigation Analysis (DRAMA) Tool*, Final Report, ESA/ESOC Contract No. 16966/02/D/HK, QinetiQ, United Kingdom

3. Rochelle W.C., Kirk B.S., Ting B.C., (1999). *User's Guide for Object Reentry Analysis Tool (ORSAT) - Version 5.0*, Volume 1, JSC-28742, NASA Lyndon B. Johnson Space Center, Houston (TX), USA

4. Astos Solutions GmbH, (2012). *ASTOS 7: Safety and Debris Risk Assessment Tutorial, ASTOS version 7.0.3*

5. Weikert S., Scholz T., Cremaschi F., (2010). *Safety and Risk Analysis Capabilities of ASTOS*, Presented at the Fourth International Conference on Astrodynamics Tools and Techniques, May 3–6, 2010, Madrid, Spain

6. Omaly P., Spel M. (2012). DEBRISK, a Tool for Re-Entry Risk Analysis, *Proceedings of the Fifth IAASS Conference*, ESA SP-699, ESA Communications, Noordwijk, The Netherlands

7. Ailor W., Hallman W., Steckel G., Weaver M., (2005). Analysis of Reentered Debris and Implications for Survivability Modeling, *Proceedings of Fourth European Conference on Space Debris*, ESA SP-587, ESA Publications Devision, Noordwijk, The Netherlands, pp. 539–544

8. Vallado D.A., Crawford P., Hujsak R., Kelso T.S., (2006). *Revisiting Spacetrack Report #3*, AIAA 2006-6753, presented at the AIAA/AAS Astrodynamics Specialist Conference, Keystone, CO, USA (available on http://celestrak.com/publications/AIAA/2006-6753/)